

# Ab initio Investigation of Elasticity and Stability of metal Aluminum

W eixue Li     T zuchiang W ang

LNM , Institute of Mechanics, China Academy of Science, Beijing, 100080, China

Based on pseudopotential plane-wave (PP-PW) method in combination with the local-density-functional theory (LDF T), the whole stress-strain curve of uniaxial loading and uniaxial deformation along [001] and [111] direction, biaxial strain proportional extension along [010] and [001] of metal Al are obtained. During uniaxial loading, general behaviors of energy vs. stretch and load vs. stretch are considered. There exist three special unstressed structures under the uniaxial loading, *f.c.c.*, *b.c.c.* and *f.c.t.* for [001]; *f.c.c.*, *s.c.* and *b.c.c.* for [111] respectively. With stability criteria, we find all of these state is unstable and always accompany with shear instability except natural *f.c.c.* structure. Bain transformation from stable *f.c.c.* structure to stable *b.c.c.* conformation cannot be obtained by uniaxial compression along any equivalent [001] and [111] direction. The tensile and compressive strength are got along both direction. Better ductility and strength is got at the [111] direction. With ratio increment of biaxial proportional extension, the stress and tensile strength increase respectively; however, the critical strain does not change significantly.

62.20.-x, 62.20.Dc, 62.20.Fe, 81.40.Jj

## I. INTRODUCTION

Investigation of elastic behavior of perfect single crystal under load is a very interesting issue. It can be applied to system in which large, elastic (but not necessary linear) deformation may occur, in case which large deformation may occur either without significant dislocation movement or before deformation by dislocation movement become dominant. Deformation of whisker, twinning, martensitic transformations are relevant examples. The instability and branching under large homogeneous strains is related to ideal strength and transformation. These informations are very useful in the analysis of structural response in solids, e. g. polymorphism, amorphization, and melting to fracture.

Born<sup>[1]</sup> criteria is widely used in investigation of strength. However, they are only valid under zero load. Based on a series of comprehensive theoretical and computational studies, Hill and Milstein<sup>[2] [7]</sup> pointed out: stability is relative and coordinate dependent; different choices of strain measure lead to different domains of stability. With this view, they investigated mechanical response of perfect crystal under different loading modes, which included the stress-strain relation, instability, branching and strength of *f.c.c.* Cu<sup>[8]</sup>, -Fe<sup>[9]</sup> and *f.c.c.* Ni<sup>[10]; [11]; [12]</sup> under uniaxial loading, uniaxial deformation and shear loading based on Morse potential. Loading direction, which they adopted, included [001], [110] and [111]. Possible transformation path were revealed. Based on thermodynamics Gibbs function, Wang<sup>[13]; [14]</sup> developed an equivalent stability analysis method and investigated the onset of instability in homogeneous lattice under critical loading. The onset modes, derived from the stability criteria, were verified by their molecular dynamics simulation. Zhou<sup>[15]</sup> derived general expression for stability criteria by constructing appropriate thermodynamics potential. Senoo et al.<sup>[16]</sup> discussed the elastic deformation of [100] loading of Al by pseudopotential method. However, the stability analysis was not done explicitly yet. He postulated that a *b.c.c.* structure could occur during [100] tension by shear branching and didn't give further proof.

Relative investigation based on the first principle is comparable less. Esposito et al.<sup>[17]</sup> deal with *f.c.c.* Cu tensile strength under uniaxial deformation based on the method of ab initio potential, augmented spherical wave (ASW) method and KKR. However, crystal structure was not permitted relaxation. Paxton et al.<sup>[18]</sup> calculated theoretical strength of *b.c.c.* transition metal, and Ir, Cu, and Al by ideal twin stress with full-potential linear muffin-tin orbital (FP-LMTO). The general response under uniaxial loading was not considered. Sob et al.<sup>[19]</sup> investigated theoretical tensile stress in tungsten single crystal under [001] and [111] loading by FP-LMTO. However, the stability analysis was not given explicitly.

Bain transformation takes a crystal from its stable *b.c.c.* conformation into a stable *f.c.c.* structure, or vice versa by means of homogeneous axial deformations. Which path requires the lowest energy and stress barrier between these states is investigated and reviewed by Milstein et al.<sup>[20]</sup>. The general mechanics and energetics of Bain transformation are presented. Based on the empirical pseudopotential, Milstein et al.<sup>[20]</sup> investigated Bain transformation of sodium crystal Na in details. Studies of this kind of transformation are also related with the investigation of epitaxial thin film<sup>[21]</sup>.

In present paper, we give a direct investigation on the elasticity, the stress-strain relation, the stability and the ideal strength of prototype metal *f.c.c.* Al with density functional theory. The stability analysis is considered explicitly

based on the theory of Hill and Mielstein [2]; [3]; [7] and Wang et al. [13]; [14]. We consider several loading modes: uniform uniaxial deformation and uniaxial loading along [001] and [111] direction, and biaxial proportional extension along [001] and [010]. The deformation is homogeneous, elastic and permitted to sufficient large. The stress-strain relation are calculated, and ideal strength is approached by loss of stability. Branching or structure transformation from a primary path of deformation takes place with the loss or exchange of stability. In this way, the mechanical response under different loading modes and direction, based on the first principle, is got clearly. With these result, Bain transformation of Al is discussed.

The paper is organized as follows. The calculation model is presented in Sec. II. In this section, we give the formulation of stress, elastic stiffness coefficients and stability criteria, especially three loading modes. Numerical precision is considered at the end of this section. As benchmark, equilibrium properties and elastic constants are calculated in the Sec. III. The [001] deformation and [001] loading is presented in Sec. IV, and stability analysis is implemented. In Sec. V, the [111] deformation and [111] loading are considered. Result of the biaxial proportional extension are given in Sec. VI. Summary and conclusion are given in Sec. VII.

## II. FORMULATION

Consider an initial unstressed and unstrained configuration, denoted as  $X_0$ . It undergoes homogeneous deformation under uniform applied load, and changes from  $X_0$  to  $X = JX_0$ , where  $J$  is the deformation gradient or the Jacobian matrix and the part of rotation is subtracted. The associated Lagrangian strain tensor is:

$$= \frac{1}{2} (J^T J - I) \quad (1)$$

and the physical strain is:

$$= (J^T J)^{\frac{1}{2}} - I \quad (2)$$

For the present deformation, internal energy  $U$  is rotationally invariant and therefore only function of  $\epsilon$ . The second Piola-Kirchhoff stress tensor  $T$  [22] is defined as:

$$T_{ij} = \frac{1}{V_0} \frac{\partial U}{\partial \epsilon_{ij}} \quad (3)$$

It relates Cauchy stress, i.e., true stress with the following equation:

$$T_{ij} = \det J J_{ik}^{-1} J_{jl}^{-1} \sigma_{kl} \quad (4)$$

where  $\det J J$  is the ratio  $V=V_0$ . With Cauchy stress, the applied force can be got by multiplying current transverse area.

At stressed state  $X$ , the elastic constants is determined through equation:

$$C_{ijkl}(X) = \frac{1}{V(X)} \left( \frac{\partial^2 U}{\partial \epsilon_{ij} \partial \epsilon_{kl}} \right)_{j^0=0} \quad (5)$$

where  $\epsilon^0$  is Lagrangian strain around the state  $X$ . These elastic constants are symmetric with interchange of indices and often expressed in condensed Voigt notation.

To analyze the stability, elastic stiffness coefficient  $B$  [14] is introduced as following:

$$B_{ijkl} = C_{ijkl} + \frac{1}{2} (\epsilon_{ik} \epsilon_{jl} + \epsilon_{jk} \epsilon_{il} + \epsilon_{il} \epsilon_{jk} + \epsilon_{jl} \epsilon_{ik} - 2 \epsilon_{kl} \epsilon_{ij}) \quad (6)$$

From this definition, we can see that  $B$  does not possess (ij) ! (kl) symmetry generally. The system may be unstable when

$$\det B = 0 \quad (7)$$

for the first time.

The following loading modes are considered:

- (i) Uniaxial Deformation.

$$\epsilon_{ij} = \epsilon_{ij} - \epsilon_{ij}^0 \quad i, j = 1, 2, 3 \quad (8)$$

In this mode, we specify a strain, and get strain energy by subtracting reference energy, which is calculated at the theoretical lattice constant, based on the total energy calculation. The respective stretches of three axes are:  $\epsilon_1 = \epsilon_2 = 1$ ,  $\epsilon_3 < 1$  for compression and  $\epsilon_3 > 1$  for tension.

(ii) Uniaxial Loading.

$$\epsilon_{ij} = \epsilon_{ij} - \epsilon_{ij}^0 \quad i, j = 1, 2, 3 \quad (9)$$

To realize the uniaxial loading, volume relaxation should be considered. In present case, we varies transverse contraction at each longitude strain and find it minimum, which corresponds zero stress on lateral faces. For crystal symmetry, the transverse contraction is same at two transverse directions. With longitude strain and respective transverse strain, strain energy of uniaxial loading is calculated. The respective stretch of three axial is: for compression,  $\epsilon_1 = \epsilon_2 > 1$ , and  $\epsilon_3 < 1$ ; for tension,  $\epsilon_1 = \epsilon_2 < 1$ , and  $\epsilon_3 > 1$ .

(iii) Biaxial Strain Proportional Extension

$$\epsilon_{22} = \epsilon_{33} = 0 \quad \epsilon_{ij} = 0 \quad \text{others} \quad (10)$$

Ab initio pseudopotential plane-wave method is implemented. Based on the mechanism of Hamman<sup>[27]</sup> and Troullier<sup>[28]</sup>, soft first principle pseudopotential are generated by package DgnppB<sup>[24]; [25]</sup>. The package Fhi96md<sup>[26]</sup>, which perform DFT total-energy calculation, employs first-principle pseudopotentials and a plane-wave basis set. In our calculations, local density approximation (LDA) with the exchange and correlation energy functional developed by Perdew and Zunger<sup>[29]</sup> is adopted.

Two supercell are designed in our calculations: one is 4-atom supercell for the equilibrium properties and elastic constants, uniaxial deformation and loading along [001], and biaxial deformation along [010] and [001]; another one is 3-atom supercell for uniaxial loading and deformation along [111]. For numerical differential feature of stress and elastic constants, the precision must be considered carefully.  $E_{\text{cut}} = 12 \text{ Ry}$  is sufficient in pseudopotential plane-wave calculation. Due to discontinuous feature of occupation number of metal electron, a large number of k-space sample must be used to reach sufficient precision. A smearing parameter are introduced to decrease the number of k-points. Our calculation show that  $\epsilon = 0.058 \text{ Ry}$  already give a satisfactory result. The respective k-mesh is  $8 \times 8 \times 8$  for 4-atom supercell, and  $10 \times 10 \times 6$  for 3-atom supercell.

### III. EQUILIBRIUM PROPERTIES AND ELASTIC CONSTANTS

As test, we have calculated the equilibrium lattice constant, elastic constants of bulk Al. F.c.c. Al has three independent elastic constant, i.e:  $C_{11}, C_{12}, C_{44}$ . The equilibrium lattice constants  $a_0$ , the bulk modulus  $B_0$ , are obtained by fitting energy-volume curve to Murnaghan equation of state.<sup>[30]</sup> The relation between bulk modulus  $B_0$  and elastic constant is  $B_0 = (C_{11} + 2C_{12})/3$ . From uniaxial deformation along [001] direction and trigonal strain along [111],  $C_{11}$  and  $C_{44}$  is obtained. The result are given in Table I.

The lattice constant,  $a_0 = 3.97 \text{ \AA}$ , is 2% smaller than experimental value  $a_0 = 4.05 \text{ \AA}$ , and respective elastic constants are 10% larger than experimental values. This difference is typical of DFT-LDA calculation and can be see clearly from other first principle results. Sun et al.<sup>[31]</sup> pointed out the elastic constants and shear modulus is sensitive to the lattice constant of crystal, and calculated it with experimental values of room temperature. Besides the elastic constants with experimental lattice constant, Mehl and Boyer<sup>[32]</sup> also gave the Bulk modulus, Young's modulus, shear modulus, average Poisson ratio and anisotropy of isotropic materials with orientation average, based on the linear augmented plane wave (LAPW) method. We carried out similar calculation and present it in Table I. All of theoretical calculations are in well agreement with experimental data, and better result are given by our calculation. However, we perform our investigation of strength and stability at the theoretical lattice constant. Any externally imposed strain and stress should be excluded for getting accurate results.

### IV. [001] LOADING AND [001] DEFORMATION

Four-atom face-centered tetragonal supercell is designed for [001] loading and [001] deformation. [100], [010] and [001] is selected as X-axis, Y-axis and Z-axis. At initial equilibrium state, the f.c.t. structure is f.c.c. With same f.c.t. cell, we can get b.c.t. cell by rotate  $\frac{\pi}{4}$  along [001] axial. This can be see clearly from Fig. 1. Start from the unstressed f.c.c. state where  $\epsilon_1 = \epsilon_2 = \epsilon_3 = 1$ , and let axial lattice be compressed: on a prescribed path, the lattice must pass

through the state  $\epsilon_3 = \epsilon_1 = \epsilon_2 = \frac{p}{2}$  where b.c.t. becomes b.c.c.. Crystal symmetry at this stage implies that the loads are hydrostatic. Under [001] loading, since the transverse loads are always zero, the axial load must also be zero at b.c.c.. Since the load must be tensile as  $\epsilon_3 \neq 1$  and compressive as  $\epsilon_3 \neq 0$ , the existence of two zeroes on the primary path of [001] loading also implies third zero in general. The third unstressed evidently does not have any higher symmetry than tetragonal. The state located at central zero is always unstable for its local energy maximum. The details analysis and proof about the general form of energy vs. stretch and stress vs. stretch should be referred to the original paper of Milstein [34].

For tetragonal symmetry of crystal under load, independent elastic constants are reduced to six as:  $C_{33}, C_{12}, C_{13} = C_{23}, C_{11} = C_{22}, C_{44} = C_{55}$  and  $C_{66}$ ; all the other  $C_{ij}$  are equal to zero. Because it is more interesting to uniaxial loading, we just analyze its stability. With equation 6, 7 and 9, we write the instability criteria as following:

$$(C_{11} + \frac{1}{2}C_{12}) - 2C_{13}(C_{13} - \frac{1}{2}C_{12}) = 0 \quad (11)$$

$$C_{11} - C_{12} = 0 \quad (12)$$

$$C_{44} + \frac{1}{2}C_{66} = 0 \quad (13)$$

$$C_{66} = 0 \quad (14)$$

The first one involves the vanishing of bulk modulus, and is referred to as spinodal instability. The second instability involves symmetry breaking (bifurcation) with volume conservation; it may be identified as the tetragonal shear breaking and referred as Born instability. With Born instability, the crystal can branch from the tetragonal path to a face-centered orthorhombic path under uniaxial dead loading; that is, the branching is  $\epsilon_1 = \epsilon_2 \neq 0$  with  $\epsilon_3 = 0$  and  $\epsilon_{11} = \epsilon_{22} = \epsilon_{33} = 0$ . The condition  $C_{66} = 0$ , when the  $C_{ij}$  are reckoned relative to the f.c.t. crystal axes, is equivalent to  $C_{11} - C_{12} = 0$  when the  $C_{ij}$  are computed relative to the axes of the b.c.t. cell. So, at state  $C_{66} = 0$  (referred to the f.c.t. axes), the tetragonal crystal branch to a body-centered orthorhombic path under uniaxial loading.  $C_{44} + \frac{1}{2}C_{66} = 0$  is another shear instability.

Energy vs. strain curve is given in Fig.2 (Without other statement, the strain, force and stress, given in figures, is physical strain, applied force and Cauchy stress.) There exist only one energy minimum under uniaxial deformation. Any departure from the minimum under this loading mode lead the rapid increment of strain energy. For the triaxial stress of uniaxial deformation, its strain energy is always great than uniaxial loading. This is same with Milstein conclusion: the uniaxial loading is lowest energy path between any Bain path. However, another local maximum and local minimum state are found under uniaxial compression. The longitude and transverse strain at local maximum is  $\epsilon_{33} = \frac{p}{2} = 0.20$  and  $\epsilon_{11} = 0.1313$  respectively; the ratio of stretch  $(1 + 0.2) = (1 + 0.1313) = 0.7071$  is approximately equal to  $1/\sqrt{2}$ . The respective structure is b.c.c. with lattice constant 3.176 Å, just like expected. The left local minimum is a f.c.t. structure with  $\epsilon_{33} = -0.305$ . From Fig.2b, we see that all of three extreme are stress free. Because b.c.c. locates at local maximum, it is always unstable.

The elastic constants and respective stability range are calculated and given in Fig. 3.  $C_{66}$  is always negative at range [-0.40, -0.128], which include the unstressed f.c.t. state. That means, although stress free f.c.t. is at the local minimum of uniaxial loading, it is still unstable to shear loading. Based on the explanation of  $C_{66}$ , this f.c.t. state can transform body-centered orthorhombic under uniaxial compression. Range of spinodal instability under compression is [-0.263, -0.119]. B.c.c. state falls in double instability.

From Fig.2b, the compressive strength of [001] loading is -5.62 GPa with  $\epsilon_{33} = -0.1$ . During tension, the stress approaches its maximum 12.54 GPa with  $\epsilon_{33} = 0.36$ . However,  $C_{11} - C_{12}$  and  $C_{44} + \frac{1}{2}C_{66}$  have already become negative when  $\epsilon_{33} > 0.272$ . Respective stress is 12.1 GPa. This gives the lower limit of tensile strength. Two branching are triggered at this critical strain. With  $C_{11} - C_{12} = 0$ , tetragonal lattice will transform into body-centered orthorhombic path and become a stable b.c.c. state at last [35]. With  $C_{44} + \frac{1}{2}C_{66} = 0$ , orthorhombic symmetry will be lost. However, which branching will take place depends on higher order elastic modulus. By means of pseudopotential methods based on the model potential proposed by Senoo [16], he got compressive strength approximately -5. GPa with strain -0.11, and unstressed b.c.c. structure occurred at strain -0.2. These results are very similar with us. However, the tensile strength, which they got, 17.4 GPa with strain 0.42 is great than ours. The  $C_{11} - C_{12} = 0$  branching was assumed to take place at strain 0.15 in their work. Paxton [18] calculated the ideal twin stress of Al based on the FP-LMTO method. The respective value,  $0.14 \frac{1}{3}(C_{11} - C_{12} + C_{44}) = 4.61$  GPa (here  $C_{ij}$  is elastic constants at theoretical lattice), is approximately one third of our tensile strength.

Unlike Ni [10]; [11]; [12] and Cu [8], -Fe [9] calculated by Milstein, uniaxial stress and force of Al is always lower than the uniaxial deformation before they approach the maximum. The transverse strain vs. longitude strain is given in Fig. 4, and the respective Poisson ratio is positive under whole uniaxial loading.

In this loading modes, supercell is designed as following: two planar vectors are identical to two primitive f.c.c. lattice, for instance along [110] and [011] direction; the third lattice vectors is in the [111] direction, here we select three layers. In each plane, there is only one atom, and three atom supercell is got.

The considered path of deformation is axisymmetric, in that all direction transverse to [111] are equally stretched or xed. The axisymmetric path of deformation under [111] loading and [111] deformation consequently passes through three cubic con guration: f.c.c., s.c. and b.c.c. with increment of compression. To illustrate this, we define a single quantity,  $r$ , the ratio of axial to transverse stretch under loading. Three smallest tetrahedron are cut separately from f.c.c., s.c., and b.c.c. shown in Fig.5. The bottom plane  $ABC$  is just  $\bar{1}11$ g plane, and the direction of  $OD$  is [111]. The ratio of height and edge length of bottom plane is  $\frac{\sqrt{6}}{3}, \frac{\sqrt{6}}{6}, \frac{\sqrt{6}}{12}$ , i. e. 1, 0.5, 0.25. This ratios is just  $r$ , which we define before. When  $r$  decreases from 1 to 0.25 during compression, the cubic f.c.c., s.c. and b.c.c. structure take place. The details can be found from Fig.5. During [111] loading, the transverse load is always zero, and cubic symmetry requires three cubic con guration is stress-free. However, during [111] deformation, the transverse load always exist, and cubic symmetry leads cubic state s.c. and b.c.c. is hydrostatic compression. For the transverse contraction under [111] loading, s.c. and b.c.c. will occur earlier than [111] deformation.

The calculated results are given in Fig.6. Just like the [001] case, there just exist one minimum under the uniaxial deformation, and the strain energy is always higher than uniaxial loading. Under uniaxial loading, another local maximum and local minimum are also found, the form of energy vs. stretch is just same as [001] loading. With Fig. 4, we get  $\epsilon_{11} = 0.334$  at the local maximum point with  $\epsilon_{33} = -0.333$ , the respective  $r$ , 0.5, just corresponds the unstressed s.c. con guration. This state is unstable for its feature of local energy maximum. At the local minimum,  $\epsilon_{11} = -0.64$  and  $\epsilon_{33} = -0.59$ , the respective  $r$ , 0.25, corresponds to unstressed b.c.c. structure. With simple geometry calculation, we get the lattice constant of stress free s.c. and b.c.c. structure 2.648Å and 3.253Å respectively. The relative elastic constants is: to s.c. :  $C_{11} + C_{12} = 10.1$  GPa,  $C_{11} - C_{12} = 24.9$  GPa and  $C_{44} = 4.4$  GPa; to b.c.c.  $C_{11} + C_{12} = 65.19$  GPa, and  $C_{11} - C_{12} = 48.92$  GPa and  $C_{44} = 26.7$  GPa. From these figures, we see that both of s.c. and b.c.c. is unstable even b.c.c. located at the local minimum of uniaxial loading. The shear instability is always along with the unstressed s.c. and b.c.c. state. Based on present and previous discussion, we conclude that for f.c.c. Al, the stable b.c.c. structure can not be got by uniaxial compression along any equivalent [001] and [111] direction. Possible Bain transformation from stable f.c.c. to stable b.c.c. is branching from uniaxial tension.

The response of nickel under [111]<sup>[12]</sup> loading was investigated in details by Milstein et al.. Based on empirical Morse functions, they studied the stability of crystal under load conveniently. For numerical feature of the first principle calculation, we just test several special points, i.e: initial f.c.c., unstressed s.c. and b.c.c. The stability of other points is not analyzed. Under this direction, the stress and force of uniaxial loading is always small than the uniaxial deformation. The maximum of tensile stress is 11.05 GPa at  $\epsilon_{33} = 0.295$ , and the maximum magnitude of compressive stress is 15.89 GPa at  $\epsilon_{33} = -0.177$ . The tensile strength and critical strain is similar with [001] tension; however the compressive strength is significantly different from the [001] uniaxial compression. The details are given in Table II. From this table, we find that better ductility and strength can be got along [111] direction.

This can be also see clearly from the following comparison. Under [001] loading, the stress free b.c.c. and f.c.t. is approached at  $\epsilon_{33} = 0.2$  and  $\epsilon_{33} = -0.305$ , where f.c.t. is local minimum and initial f.c.c. is overall minimum. The energy barrier from these minimums is given as following:  $E_{f.c.c. \rightarrow f.c.t.} = 0.1047$  (ev/atom),  $E_{f.c.c. \rightarrow f.c.c.} = 0.0319$  (ev/atom). At the [111] loading, strain of unstressed s.c. and b.c.c. con guration is -0.333 and -0.59, where b.c.c. is local minimum. The respective energy barrier is:  $E_{f.c.c. \rightarrow b.c.c.} = 0.3766$  (ev/atom),  $E_{b.c.c. \rightarrow f.c.c.} = 0.2766$  (ev/atom). Higher energy transition barrier and critical strain is needed under [111] compression.

## V I. B I A X I A L S T R A I N P R O P O R T I O N A L E X T E N S I O N

Biaxial strain proportional extension is considered here. In present paper, we deal with extension along [010] and [001] direction, and do not consider volume relaxation. The stability analysis of this mode is also neglected for the illustration purpose.

The strain ratio between [010] and [001] is 0.25, 0.5 0.75 and 1. The result is given in Fig.7. With increment of ratio, the energy, stress and maximum stress increases, respectively. The reason is straightforward: more energy is needed with a higher transverse strain at the same longitude strain. However, the critical strain is similar at different proportional loading modes.

## VII. SUMMARY AND CONCLUSION

Based on the DFT total energy calculation and stability theory, we give a detail investigation of mechanical response of f.c.c. Al under different loading modes and loading direction. We get the following conclusions:

(1). Due to the requirement of crystal symmetry, a general form of energy vs. stretch and stress vs. stretch under uniaxial loading of cubic crystal will be presented: one local minimum, one local maximum and one overall minimum for energy vs. stretch curve, which relate with three unstressed state. The state, stand intermediate of three extreme, is always unstable for its feature of energy maximum.

However, when we consider the more complicated crystal, for example diamond structure or alloys<sup>[36]; [37]</sup>, the above conclusion should be carefully examined. At this time, the symmetry is determined by both the structural parameters and atomic ordering, and some symmetry-dictated extreme may be lost.

(2). The whole stress-strain curve of uniaxial deformation and uniaxial loading along [001] and [111] direction, and biaxial proportional extension are got. The magnitude of stress and force of uniaxial deformation is always great than the uniaxial loading at [001] and [111] direction. The stability range of [001] loading is explicitly given out. The tensile and compressive strength along [001] and [111] direction are obtained.

(3). Under path of [001] loading, the local minimum, local maximum and overall minimum correspond unstressed f.c.t., b.c.c. and f.c.c.; under [111] loading, they relates stress free state b.c.c., s.c. and f.c.c. respectively. The intermediate b.c.c. at [001] loading and s.c. at [111] loading is unstable. Although the f.c.t. at [001] loading and b.c.c. at [111] loading fall in the local minimum, they are still unstable for the shear instability. Worth to point out, the b.c.c. conformation, presented at the [001] and [111] loading, is different conformation. Their lattice constants is 3.176Å and 3.253Å, and the previous locates local maximum, and the later, at local minimum.

A stable b.c.c. state of metal Al cannot be obtained by uniaxial compression along any equivalent [001] and [111] direction. Possible Bain transformation is branching from the prescribed path of uniaxial loading along equivalent [001] or [110] direction accompanied by branching.

(4). The tensile strength is similar and compressive strength is remarkable different along [001] and [111] direction. Better ductility and strength can be got at the [111] direction.

## ACKNOWLEDGMENTS

This work was supported by the NSF (Grant No.19704100). One of authors W. Li thanks Prof. D. S. Wang for a useful discussion and encouragement. One of authors W. Li also thanks Dr. Y. Yao for transferring package DgnqppB on the Linux system. Parts of computations are performed at the super-parallel computer of Network Information Center of China Academy of Science.

- 
- [1] M. Born, Proc. Cambridge Phil. Soc. 36, 160 (1940); M. Born and K. Huang, Dynamical Theory of Crystal Lattices (Clarendon, Oxford, 1956).
  - [2] R. Hill, Math. Proc. Cambridge Philos Soc. 77, 225 (1975).
  - [3] R. Hill, F. M. Ilstein, Phys. Rev. B 15, 3087 (1977).
  - [4] F. M. Ilstein and R. Hill, Phys. Rev. Lett. 43, 1411 (1979).
  - [5] Idem J. Mech. Phys. Solids 25, 457 (1977).
  - [6] Idem ibid 26, 213 (1978).
  - [7] F. M. Ilstein, in Mechanics of Solids, edited by H. K. Hopkins and M. J. Sewell (Pergamon, Oxford, 1982), p. 417.
  - [8] F. M. Ilstein, B. Farber, Phil. Mag. A 42, 19 (1980).
  - [9] F. M. Ilstein, Phys. Rev. B 3, 1130 (1971).
  - [10] F. M. Ilstein, I. Appl. Phys. 44, 3833 (1973).
  - [11] F. M. Ilstein, K. Huang, Phys. Rev. B, 18, 2529 (1978).
  - [12] F. M. Ilstein, R. Hill, K. Huang, Phys. Rev. B 21, 4282 (1980).
  - [13] J. Wang, S. Yip, S. Phillpot, and D. Wolf, Phys. Rev. Lett 77, 4182 (1993).
  - [14] J. Wang, J. Li, S. Yip, S. Phillpot and D. Wolf, Phys. Rev. B 52, 12627 (1995).
  - [15] Z. Zhou, B. Joos, Phys. Rev. B 54, 3841 (1996).
  - [16] M. Senoo, I. Fujishiro and M. Hirano, Bull. JMS 27, 2680 (1984).
  - [17] E. E. Sposito, A. E. Carlsson, D. D. Ling, H. Ehrenreich, C. D. Gelatt Jr., Phil. Mag. 41, 251 (1980).

- [18] A. T. Paxton, P. Gumbsch and M. Methfessel, *Phil. Mag. Lett.* 63, 267 (1991).
- [19] M. Sob, L. G. Wang, V. Vitek, *Mater. Sci. Engin. A* 234 – 236, 1078 (1997); P. Sandera, J. Pokluda, L. G. Wang, M. Sob, *ibid.*, A 234 – 236, 370 (1997).
- [20] F. M. Ilstein, H. Fang, and J. Marschall, *Phil. Mag. A* 70, 621 (1994).
- [21] S. Fox and H. J. F. Hansen, *Phys. Rev. B* 53, 5119 (1996).
- [22] C. Truesdell and R. Toupin, *Handbuch der Physik*, edited by S. Flugge (Springer-Verlag, Berlin, 1960), Vol. III/1, p. 226.
- [23] P. Hohenberg, and W. Kohn, *Phys. Rev.* 136, B 864 (1964); W. Kohn and L. J. Sham, *ibid.* 140, A 1133 (1965)
- [24] M. Fuchs, M. Scheer, *Comput. Phys. Commun.*, to be published
- [25] X. Gonze, R. Stumpf, M. Scheer, *Phys. Rev. B* 44, 8503 (1991).
- [26] M. Bockstedte, A. Kley, J. Neugebauer and M. Scheer, *Comput. Phys. Commun.* 107, 187 (1997).
- [27] D. R. Hamman, *Phys. Rev. B* 40, 2980 (1989).
- [28] N. Troullier, J. L. Martins, *Phys. Rev. B* 43, 1993 (1991).
- [29] J. Perdew, A. Zunger, *Phys. Rev. B* 23, 5048 (1981).
- [30] F. D. Mumaghan, *Proc. Nat. Acad. Sci. U.S.A.* 50, 697 (1944).
- [31] Y. Sun, E. Kaxiras, *Phil. Mag. A* 75, 1117 (1997).
- [32] M. J. Mehl, B. M. Klein and D. A. Papaconstantopoulos, *Intermetallic Compounds: Vol. 1, Principles*, J. H. Westbrook and R. L. Fleischer, eds. (John Wiley & Sons, Ltd., London, 1994), Ch. 9.
- [33] F. M. Ilstein, *J. Mater. Sci* 15, 1071 (1980).
- [34] F. M. Ilstein, *Solid. St. Commun.* 34, 653 (1980).
- [35] F. M. Ilstein, B. Farber, *Phys. Rev. Lett.* 44, 277 (1980).
- [36] P. J. Cralovich, M. Weinert, J. M. Sanchez, R. E. Waston, *Phys. Rev. Lett.* 72, 3076 (1994).
- [37] M. Sob, L. G. Wang, V. Vitek, *Comp. Materials. Sci.*, 8, 100 (1997).

TABLE I. Elastic modulus of Al at equilibrium state. The length unit is Å, and elastic constants unit is GPa. Here T = 0K means with theoretical lattice constant, and T = 300K with experimental lattice constant.

	$a_0$	$C_{11} + C_{12}$	$C_{11}$	$C_{12}$	$C_{44}$	B	G	E	A
Exp.	4.05	168	46	28	76.	26.	70.	0.35	1.22
Present work (T = 0K)	3.97	183	61.4	37.4					
Mehl(T = 0K) <sup>[32]</sup>	3.99	184	58.	33.					
Sun (T = 0K) <sup>[31]</sup>	3.95		58.8	45.5					
Present work (T = 300 K)	4.05	164	44.8	28.1	74.7	25.6	69.0	0.347	1.25
Mehl(T = 300 K) <sup>[32]</sup>	4.05	150	50	31	67.	28.	75.	0.31	1.24
Sun (T = 300K) <sup>[31]</sup>	4.05		45	29.7					

TABLE II. The Calculated Strength of Al under different Loading modes

	Uni. Deformation	$\sigma_{33} = \sigma_{11} = \sigma_{22}$	Uni. Loading	$\sigma_{33} = \sigma_{11} = \sigma_{22}$
[001] tensile strength (GPa)	12.65	0.30, 0.	12.1	0.272, -0.0386
[001] compressive strength (GPa)			-5.62	-0.1, 0.049
[111] tensile strength (GPa)	11.52	0.265, 0.	11.05	0.295, -0.0453
[111] compressive strength (GPa)			-15.89	-0.177, 0.110
Shear strength (GPa)	4.61	Paxton <sup>[18]</sup>		



FIG .1. Two fundamental cells of the face-centered tetragonal lattice and body-centered tetragonal lattice within same lattice

FIG .2. The calculated strain energy (a), force and stress (b) during  $[001]$  deformation and  $[001]$  loading at theoretical lattice constant.

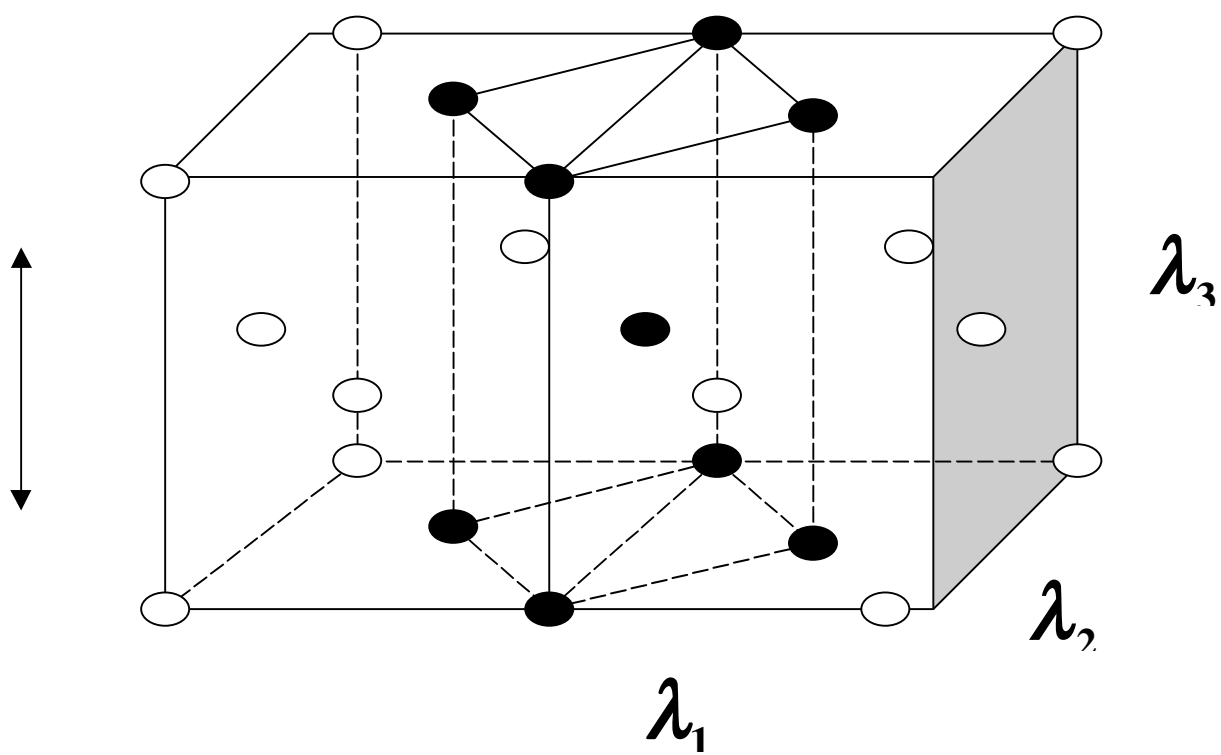
FIG .3. The calculated elastic constants (a) and stability (b) during  $[001]$  loading at theoretical lattice constant.

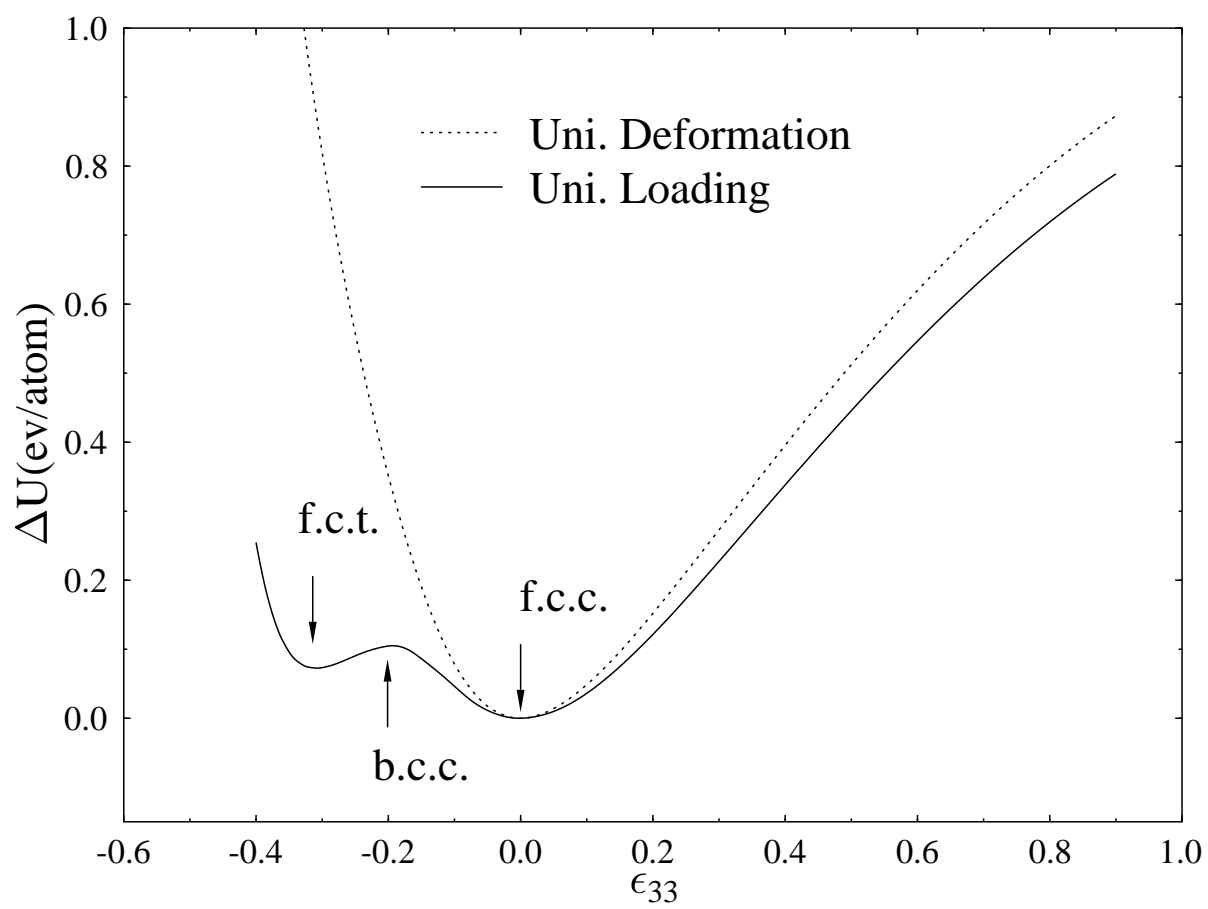
FIG .4. The calculated transverse strain of  $[001]$  loading and  $[111]$  loading at theoretical lattice constant.

FIG .5. Three smallest tetrahedron cut separately from f.c.c., s.c., and b.c.c. The length unit of each tetrahedron is its lattice constant of original lattice. Bottom plane is just  $[111]$  plane, and the triangle ABC is equilateral triangle; the direction of OD is  $[111]$ . The ratio of OD to CB is the ratio of longitude stretch to transverse stretch.

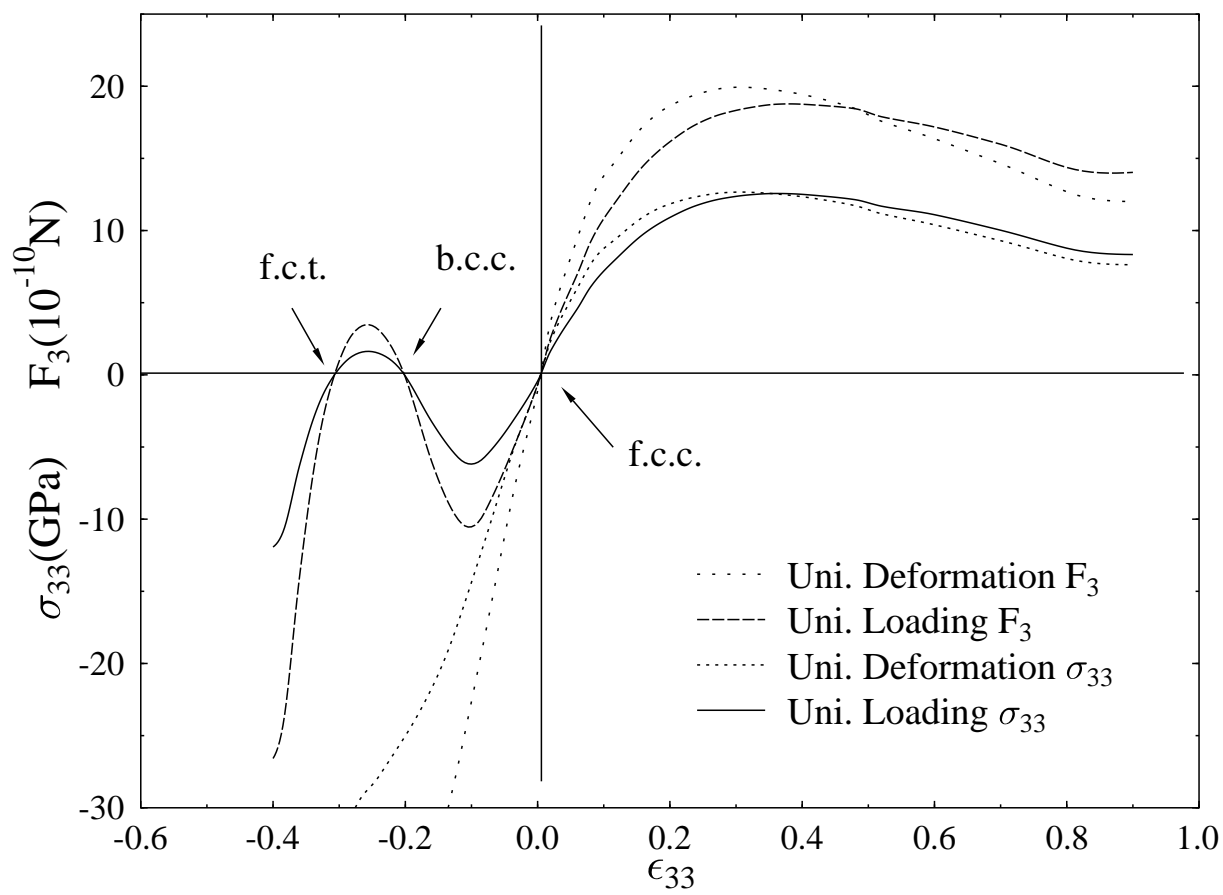
FIG .6. The calculated strain energy (a), force and stress (b) of  $[111]$  deformation and  $[111]$  loading at theoretical lattice constant.

FIG .7. The calculated strain energy (a) and stress (b) during biaxial strain proportional extension with direction ratio along  $[010]$  and  $[001]$  direction at theoretical lattice constant.

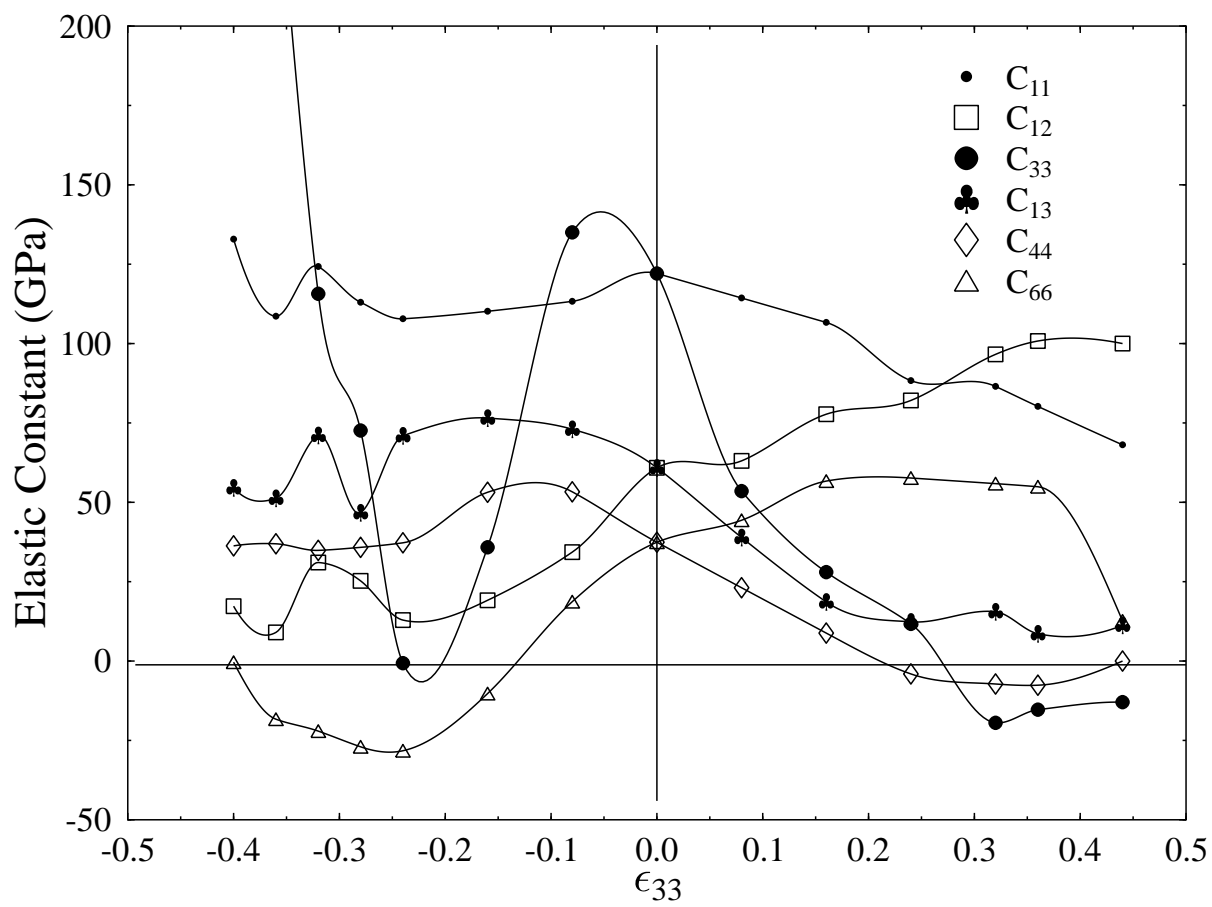




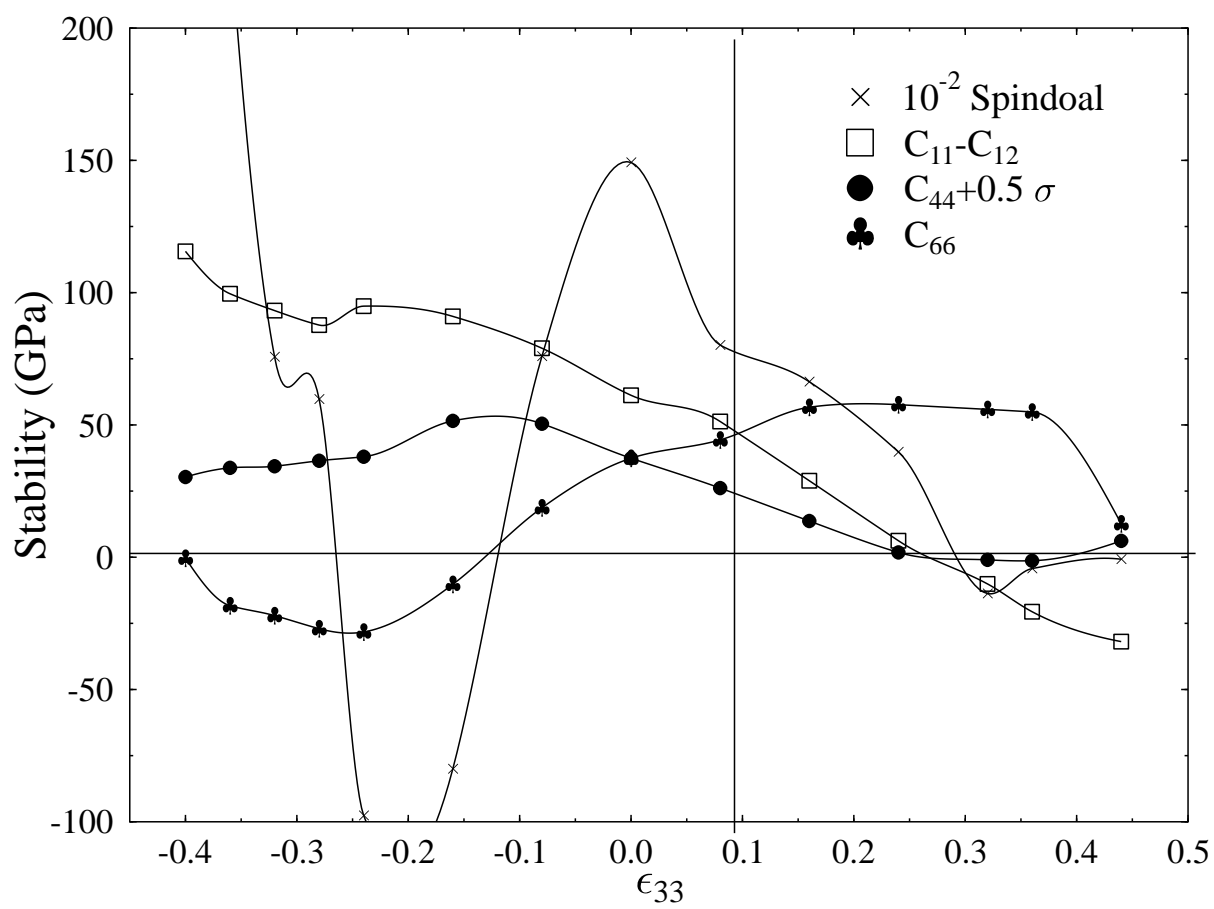
(a)



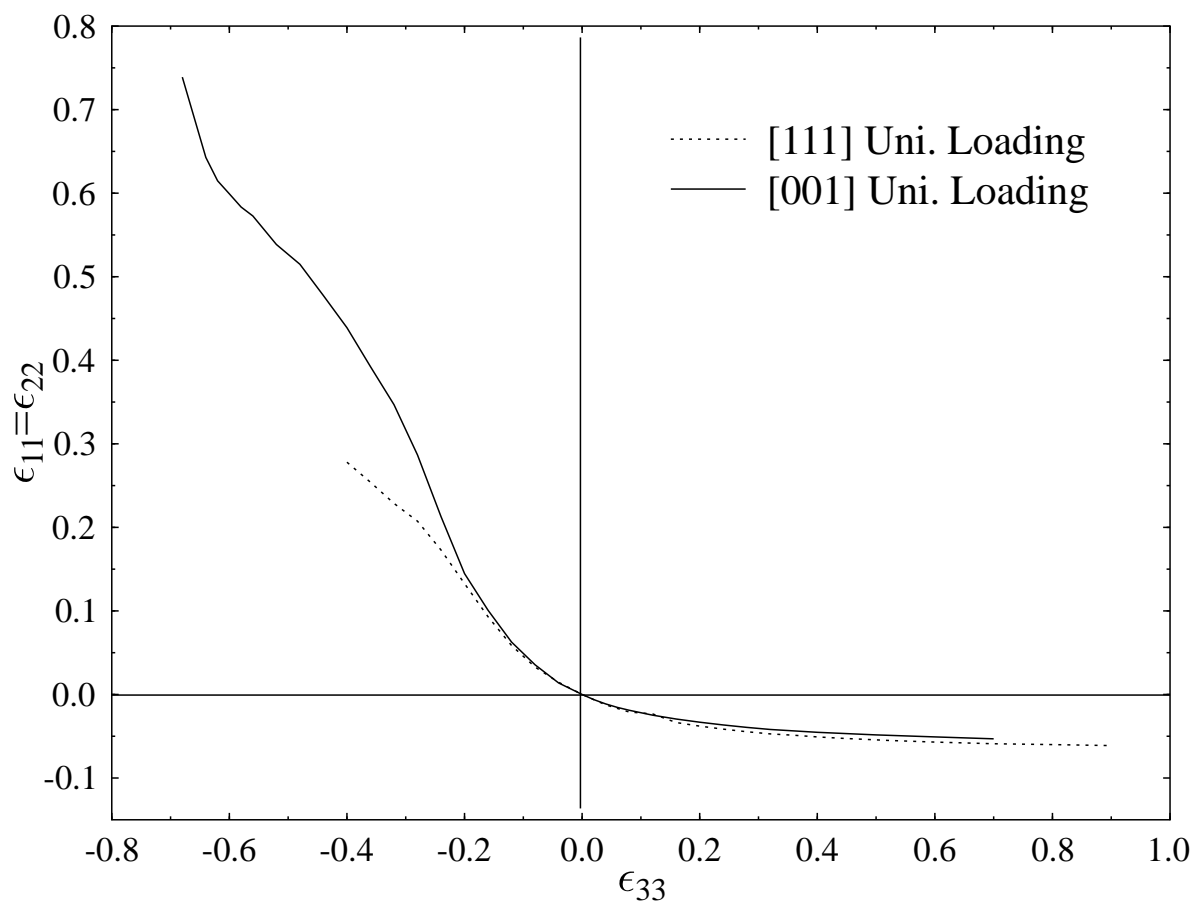
(b)

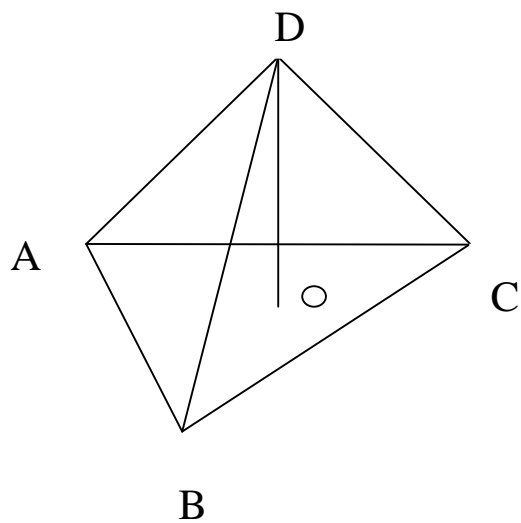


(a)



(b)



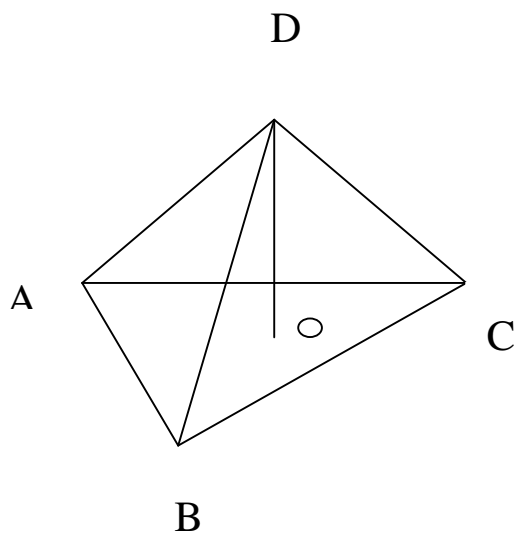


F. C. C.

$$AC = BC = AB = 2^{1/2}/2$$

$$DA = DB = DC = 2^{1/2}/2$$

$$DO/AB = 6^{1/2}/3$$

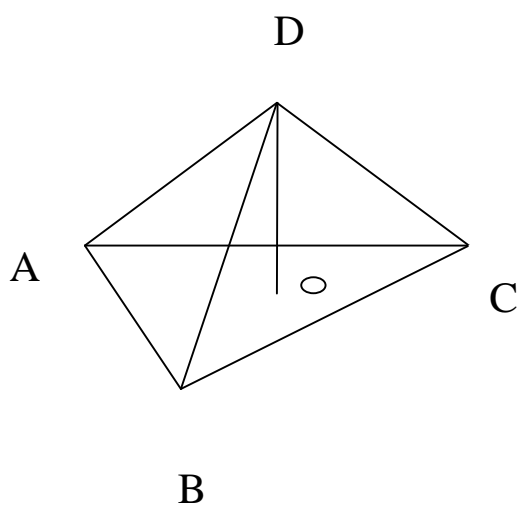


S. C.

$$AC = BC = AB = 2^{1/2}$$

$$DA = DB = DC = 1$$

$$DO/AB = 6^{1/2}/6$$



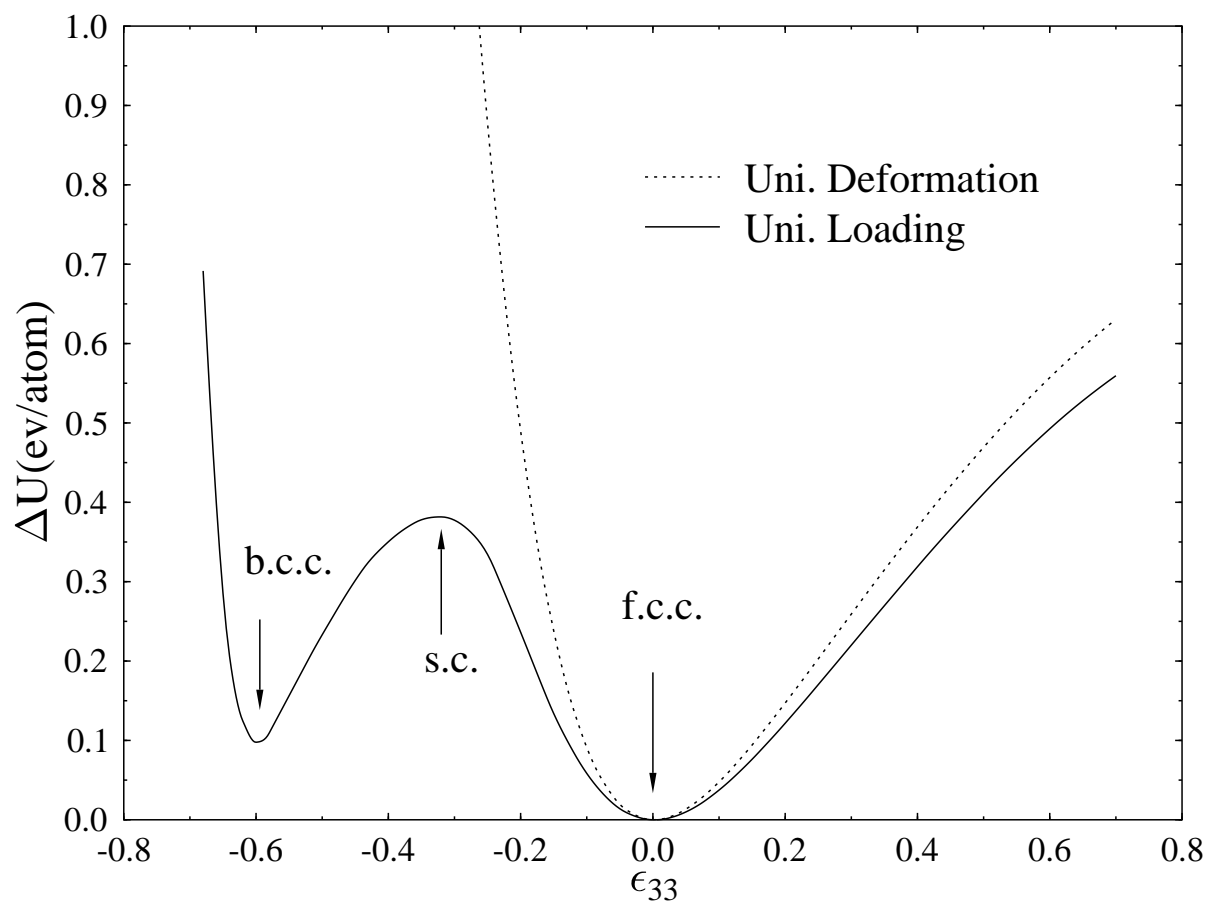
B. C. C.

$$AC = BC = AB = 2^{1/2}$$

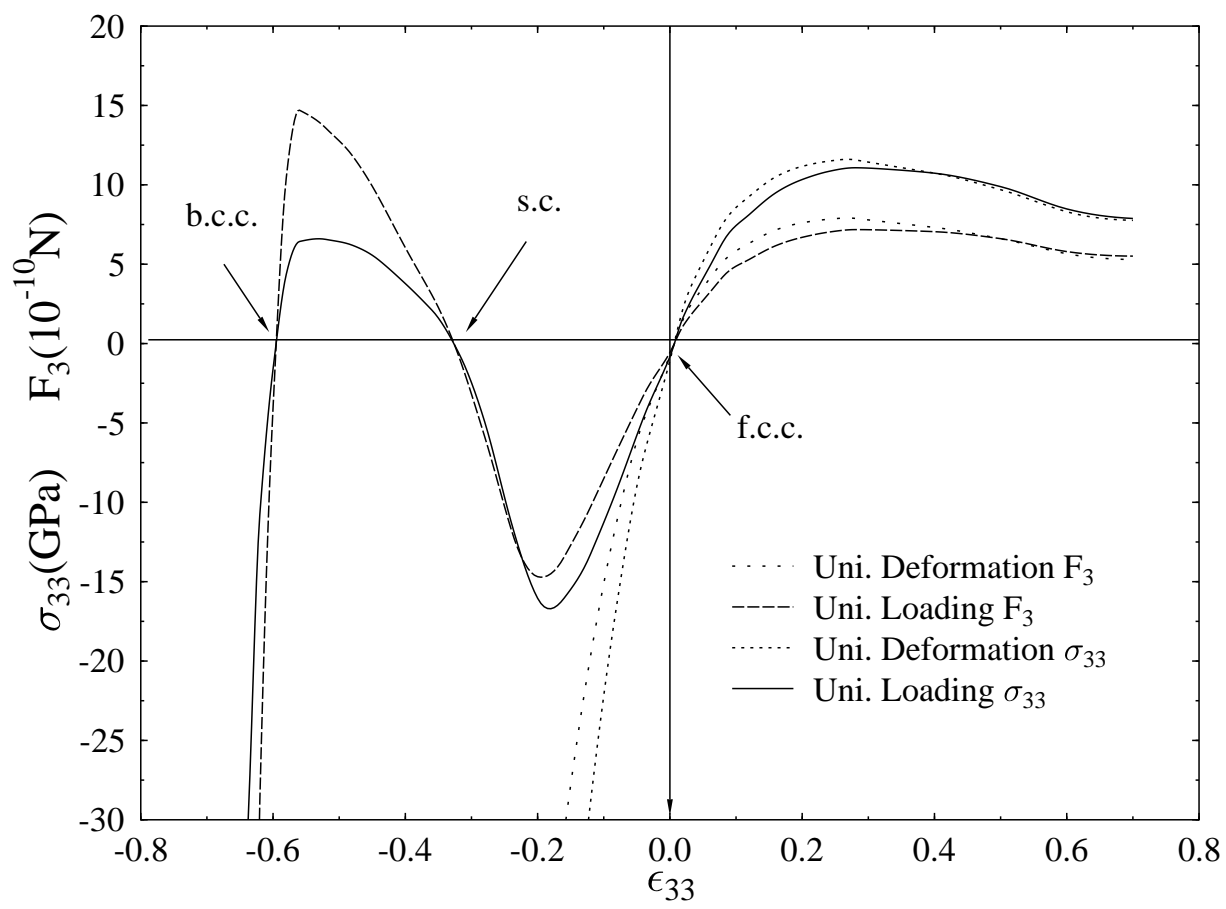
$$DA = DB = DC = 3^{1/2}/2$$

$$DO/AB = 6^{1/2}/12$$

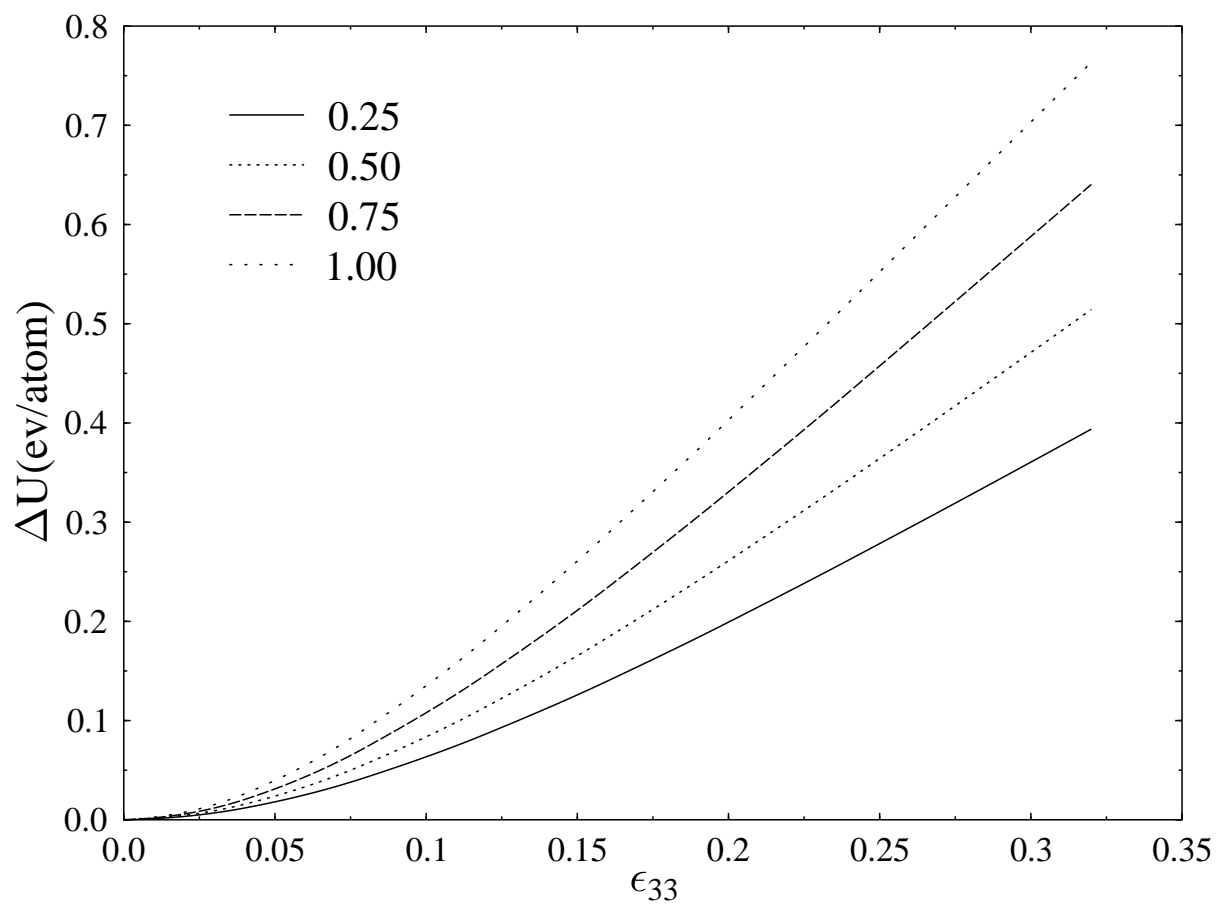




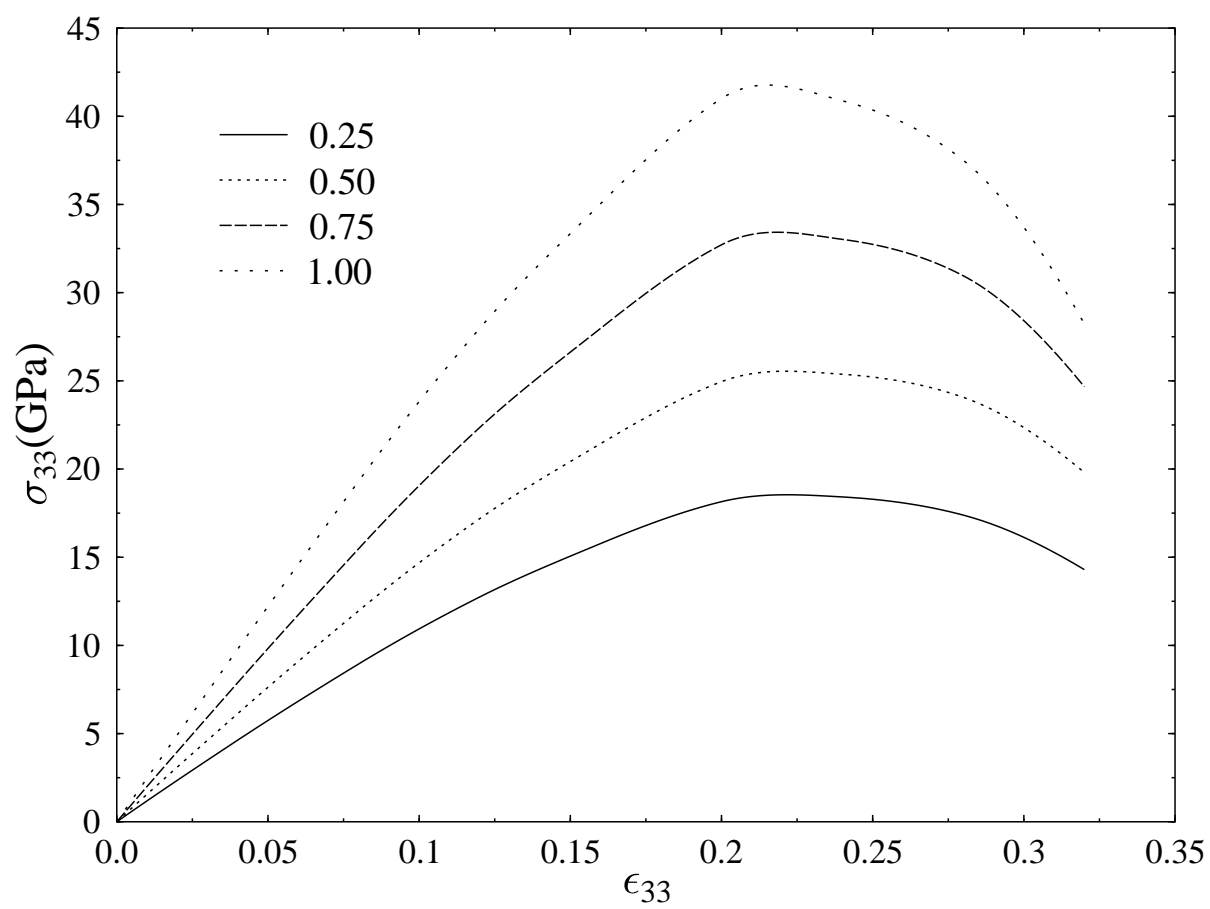
(a)



(b)



(a)



(b)